

# Pulsar Timing Arrays and Gravity Tests in the Radiative Regime

K J Lee<sup>1</sup>

<sup>1</sup> Max-Planck-Institut für Radioastronomie, Auf dem Hügel 69, D-53121 Bonn, Germany

E-mail: kjlee007@gmail.com

**Abstract.** In this paper, we focus on testing gravity theories in the radiative regime using pulsar timing array observations. After reviewing current techniques to measure the dispersion and alternative polarization of gravitational waves, we extend the framework to the most general situations, where the combinations of a massive graviton and alternative polarization modes are considered. The atlas of the Hellings-Downs functions is completed by the new calculations for these dispersive alternative polarization modes. We find that each mode and corresponding graviton mass introduce characteristic features in the Hellings-Downs function. Thus, in principal, we can not only detect each polarization mode, measure the corresponding graviton mass, but also discriminate the different scenarios. In this way, we can test gravity theories in the radiative regime in a generalized fashion, and such method is a direct experiment, where one can address the gauge symmetry of the gravity theories in their linearised limits. Although current pulsar timing still lacks enough stable pulsars and sensitivity for such practices, we expect that future telescopes with larger collecting area could make such experiments be feasible.

Submitted to: *Class. Quantum Grav.*

## 1. Introduction

Pulsars are compact rotating celestial objects, which radiate beamed electromagnetic waves. Due to the rotation of pulsar, observers on the Earth will detect pulsed emissions. Because the pulsar rotation is highly stable (Verbiest et al., 2009), measuring the timing residuals, that is, the differences between observed and predicted time of arrivals (TOAs), enables one to study the processes affecting the timing. Gravitational waves (GWs) perturb the metric of space time, on which the pulse propagates. In this way, one can directly detect GWs (Estabrook and Wahlquist, 1975; Sazhin, 1978; Detweiler, 1979) using pulsar timing techniques.

In order to discriminate the GW signal from noise, one can monitor several pulsars at the same time, compare all the TOAs, and extract the common signal induced by the GW. Such a combination of simultaneous pulsar timing data is called pulsar timing array (PTA), which allows for the detection of GWs at much lower frequencies, in the nano-Hertz band. The confidence of a positive GW detection using PTAs comes from the fact that there will be characteristic correlations of the timing residuals between widely-spaced pulsars, if fluctuations of TOAs are induced by GWs. It is hard for other types of noise to mimic such spatial correlation. The pioneering work by Hellings and Downs (1983) attempted to detect this effect by cross-correlating the time derivative of the timing residuals of multiple pulsars. Jenet et al. (2005) improved the techniques by directly correlating residuals, rather than their time derivative. They also proved that detecting the stochastic GW background generated by super massive blackhole binaries (Jaffe and Backer, 2003; Wyithe and Loeb, 2003; Enoki et al., 2004; Sesana et al., 2004, 2008; Wen et al., 2009) can be feasible with cutting-edge pulsar observing systems. Many related efforts to detect GWs with PTA were proposed afterwards, which include various detection-scheduling algorithms (Anholm et al., 2009; van Haasteren et al., 2009; Burt et al., 2011; Yardley et al., 2011; Cordes and Shannon, 2012; Ellis, Siemens and Creighton, 2012; Lee et al., 2012), different types of sources such as the single continuous sources (Jenet et al., 2004; Sesana and Vecchio, 2010; Sesana et al., 2009; Deng and Finn, 2011; Lee et al., 2011; Boyle and Pen, 2012; Babak and Sesana, 2012; Ellis, Jenet and McLaughlin, 2012; Kashiyaama and Seto, 2012; Mingarelli et al., 2012), the burst sources (Finn and Lommen, 2010), the stochastic background (Sesana et al., 2008; Ravi et al., 2012; Sanidas et al., 2012), and the memory effects (Seto, 2009; van Haasteren and Levin, 2010; Cordes and Jenet, 2012), and many other applications. Readers can consult the summary by Lommen (2012) or reviews in this volume for the related references.

We can study the intrinsic properties of GWs as well as the related astrophysics via GW observations using PTAs. General relativity (GR) has been extremely successful in describing gravitational interactions, while there remains many feasible alternatives (Will, 2006). Some of these alternatives may pave the way to the final grand unification theory of four types of fundamental interactions. In this way, testing gravity theories is fundamentally important. In the PTA context, we can test gravity theories in the

radiative regime by investigating the intrinsic properties of GWs (Lee et al., 2008, 2010; Chamberlin and Siemens, 2012), e.g. measuring the polarization and dispersion of GWs. All of these efforts limit the test to the case, where either 1) an alternative polarization or 2) a graviton induced dispersion presents.

This paper is to extended previous efforts to more general situations, where we consider all the possible combinations of alternative GW polarizations and gravity induced dispersion. The structure of the paper is: In Section 2 and 3, we will review the current efforts to detect the dispersion and the polarization modes of GW beyond the prediction of GR. The extension of these work to include the more general situation is in Section 4. The conclusions and discussions are made in Section 5

## 2. Test gravity theories with GW dispersion relation

It is well known that the corresponding particles of GWs, as in the linearised theory of GR, have zero masses. Such zero-mass graviton introduces an  $1/r$  Newtonian potential in the static weak field limit, and makes the phase velocity of GWs be identical to light velocity  $c$  regardless of frequency. Introducing a non-zero graviton mass, in general, leads to a theoretical issue of the so-called vDVZ discontinuity (Iwasaki, 1970; van Dam and Veltman, 1970; Zakharov, 1970). No matter how small the graviton mass is, there exists a coupling of zero helicity state graviton, such that the gravitation induced light deflection angle becomes  $4/3$  times that of the GR prediction. At present, light bending measurements have already tested GR to a very high precision. For example, GR predicate that the post-Newtonian parameter  $\gamma = 1$ , and Fomalont et al. (2009) have confined the post-Newtonian parameter  $\gamma = 1 + (1 \pm 5) \times 10^{-4}$  by measuring the solar gravitational deflection of radio waves. However, the theories involving massive gravitons cannot be simply ruled out, because of possible mechanisms to resolve such discontinuity (Vainshtein, 1972; Visser, 1998; Deffayet et al., 2002; Damour et al., 2003; Finn and Sutton, 2002). In these mechanisms, a nonlinear contribution is usually introduced such that the theory smoothly transits to GR at zero-mass limit ‡.

There are two groups of methods to probe the graviton mass. One is to check the large scale static gravitational field, i.e. to detect the extra exponential decay of field potential (Yukawa potential) in the form of  $e^{-r/r_{\text{cut}}}$ . Here the characteristic decay length scales  $r_{\text{cut}} \propto \hbar/m_g c$  is inversely proportional to the graviton mass  $m_g$ , and the  $\hbar$  is the reduced Planck constant. No deviation so far has been found in experiments performed on various scales from sub-millimeter to galaxy cluster size (see Goldhaber and Nieto (2010) for a thorough list).

Another way to probe the graviton mass is to investigate the GW dispersion relation, i.e. the frequency dependence of the GW velocities. Such an approach has not been taken yet, since the direct detection of GWs has not yet succeeded. Because of the model dependence, one should be careful in interpreting the graviton mass in the two

‡ In fact, one must include the nonlinear corrections, e.g. it is well known that the linearised model of GR give a  $4/3$  times Mercury perihelion precession rate compared to the weak field limit.

scenarios, i.e. the Newtonian and the linear limit. The massive GW dispersion relation can be inferred by replacing the corresponding terms in the particle energy-momentum relation by their quantum versions, i.e. energy  $E \rightarrow \hbar\omega_g$  and momentum  $\mathbf{p} \rightarrow \hbar\mathbf{k}_g$ , where the  $\omega_g$  and  $\mathbf{k}_g$  are the angular frequency and wave vector of the GW. The GW dispersion relation then becomes

$$\mathbf{k}_g(\omega_g) = \frac{(\omega_g^2 - \omega_{\text{cut}}^2)^{\frac{1}{2}}}{c} \hat{\mathbf{n}}, \quad (1)$$

where  $\hat{\mathbf{n}}$  is the unit vector in the GW propagation direction. If the GW frequency  $\omega_g$  is less than the cut-off frequency  $\omega_{\text{cut}} \equiv m_g c^2 / \hbar = 3.0 \left( \frac{m_g}{10^{-23} \text{ eV}} \right) \text{ rad yr}^{-1}$ , then the wave vector becomes imaginary, and the waves attenuate on the length scale of  $r_{\text{cut}}$ . The PTA observations usually have cadence of more than a few days. In this way, there would be no GW signal in pulsar TOA, if  $m_g \geq 10^{-22} \text{ eV}$ . Up to now, in the context of PTA, only the dispersion relations like equation (1) were considered, although there are generalizations of this dispersion relation inspired by the Lorentz-violating theories or quantum theories of gravity (Mirshekari et al., 2012).

The dispersion of GWs introduces a frequency dependent phase to the wave propagation. The dispersion effect is ‘amplified’ by the source distance, since the phase is distance-dependent as  $\mathbf{k}_g(\omega_g) \cdot \mathbf{x}$ . In this way, observing the GW from a distant system and comparing to the modeled intrinsic waveform will enable one to measure the graviton mass, as demonstrated by (Will, 1998; Arun and Will, 2009; Stavridis and Will, 2009). The primary target source of PTA experiments, on the other hand, is the stochastic GW background. In this way, the method of detecting the effect of graviton mass using PTAs is very different from the above approach, where one can model the intrinsic GW waveform.

The timing residual ( $R$ ) induced by GWs can be written as the multiplication of two parts. One part describes the geometrical setups of the pulsars and the observer on the Earth, and the other part describes the GW waveform, as shown in the following equation, one can check Lee et al. (2010) for the detailed calculations.

$$R = -\frac{1}{\mathcal{S}} A^{ij} H_{ij}, \quad (2)$$

The part  $H_{ij}$  describes the GW amplitude and propagation such that

$$H_{ij} = \int_0^\tau h_{ij}(\tau, 0) - h_{ij}(\tau - |\mathbf{D}|/c, \mathbf{D}) d\tau, \quad (3)$$

and  $\mathcal{S}$  involves the dispersion relation of the GW,

$$\mathcal{S} = 2(1 + (c/\omega_g)\mathbf{k}_g \cdot \hat{\mathbf{n}}) \quad (4)$$

The part that describes the geometrical setups is

$$A^{ij} \equiv \hat{\mathbf{n}}^i \hat{\mathbf{n}}^j. \quad (5)$$

Here the observer is at the coordinate origin,  $\mathbf{D}$  is the displacement vector from the observer to the pulsar,  $\hat{\mathbf{n}}^i$  is the direction from the observer (Earth) to the photon’s source (pulsar). One can see that the spatial correlation of pulsar timing

residuals, i.e. the cross-power  $C$  between two different pulsars, is  $C_{1,2}(\theta) = \langle R_1 R_2 \rangle = A_1 A_2 \langle \mathcal{S}_1 \mathcal{S}_2 H_1 H_2 \rangle$ , where the sub-scripts are indexes for the pulsars, the  $\theta$  is the angle between the two pulsars. Clearly, the graviton mass introduces its signature in the spatial correlation of pulsar timing residuals via  $\mathcal{S}$  and  $H$ , since both depend on the dispersion relation of the GW.

We now try to understand the effects of the graviton mass in terms of such cross-power. From equation (3), one can see that

$$\lim_{\omega_g \rightarrow \omega_{\text{cut}}} R = A^{ij} \frac{1}{2} \int_0^\tau h_{ij}(\tau, 0) - h_{ij}(\tau - |\mathbf{D}|/c, 0) d\tau. \quad (6)$$

At such a limit, the cross power become  $C \propto A_1 A_2 h h$ , i.e. it is the power of the projected GW strain tensor  $h_{ij}$  onto the basis spanned by the pulsar directions. In this situation, one can expected that  $C(\theta)$  will be of  $90^\circ$  symmetry for the two transverse-traceless modes predicted by GR, i.e. the quadruple nature of the  $h_{ij}$  gives  $C(90^\circ - \theta) = C(90^\circ + \theta)$ . Apart from this limit, the  $90^\circ$  symmetry  $h_{ij}$  will not manifest in the final correlation function. This is mainly because the term  $\mathcal{S}$ , describing the wave propagation, breaks the symmetry around  $90^\circ$ .

### 3. Test gravity theories with GW polarimetry

Besides the dispersive properties, the other type of intrinsic properties helping to test gravity theories is the allowed polarization modes of the GW. It is well known that GR predicts two allowable modes, the transverse-traceless modes. One would expected that, since gravity is mediated via the spin-2 particles, the maximal number of polarization modes of GWs would be five, i.e.  $2s + 1 = 5$ , and  $s = 2$ . However, one can prove (Eardley et al., 1973; Lee et al., 2008) that six polarization modes are required to fully describe the most general polarization states of GW. The possible states are: 1) two helicity-0 modes, a transverse breathing and a longitudinal modes, 2) two helicity-1 shear modes, 3) two transverse-traceless modes. Such apparent incompatibility between the five spin states and six polarization modes lies in the assumption of the two analysis frameworks. The spin classification is based on the unitary presentation of the wave-function transforms, while the analysis for GWs was not limited to the case §.

The cross power between the timing residual of pulsar pairs depends on the angular separation of the pulsar. The so-called Hellings-Downs (HD) function is defined as the cross-correlation coefficient of the pulsar timing residuals, i.e. the cross power normalized by the signal power. The shape of HD function, taking pulsar angular separation as the argument, is sensitive to the polarization state of GWs. In this way, one can detect and differentiate the GW polarization modes by measuring the HD

§ The presentation of the little group for the GW transformation here, i.e. the subgroup of the Lorentz group keeping GW wave 4-vector invariant, is indecomposable (Dirac, 1984) in the vector space spanned by the six polarization modes (Eardley et al., 1973). Note that there is a typo in the definition of “indecomposable” in that paper.

function. The way that GW polarization enters the HD function can be seen from equation (2), where the  $H_{ij}$  is polarization dependent.

The power of pulsar timing residuals also critically depends on the GW polarization. Many authors (Lee et al., 2008; Alves and Tinto, 2011; Chamberlin and Siemens, 2012) noticed that the timing residuals induced by longitudinal GWs will be amplified by the distance from observer to the pulsars. Chamberlin and Siemens (2012) further found that certain pulsar pairs with very small angular distances can also be used to increase the sensitive of detecting longitudinal modes. The two shear modes share similar features of the longitudinal mode, although the amplifying factor is rather limited due to its logarithmic dependence on the pulsar-Earth distances. For the rest of the modes, i.e. all transverse modes, the pulsar timing responses are similar and nearly independent of the pulsar-Earth distance. One can understand such distance dependence by considering a limiting case, where the GW propagates along the line of sight of the pulsar. For the longitudinal modes, the GW and photon travel in phase, and there is a non-oscillatory contribution to the photon's red shift. Such a non-oscillatory contribution accumulates and gives an amplifying factor proportional to the pulsar distance.

The above analysis is all based on the assumption that the GW travels at the same speed as the photons. However, one would naturally expect that the alternative polarization modes could also be dispersive, especially because introducing a graviton mass would break the gauge symmetries and thus allow for those alternative polarizations to be excited. Previously, there were investigation on the pulsar timing response and cross-power for either 1) massive GR modes, or 2) massless alternative modes. To fully understand the influence of GWs on pulsar timing residuals, it is desirable to extend current works to the more general case. In next section, we will try to complete this mission by studying the pulsar timing response to these massive alternative modes.

#### 4. Pulsar timing response to massive GW stochastic background with alternative polarization modes

The HD functions for a stochastic GW background with massive gravitons are affected by the total length of the data and sampling duration (Lee et al., 2010). It seems to be impossible to analytically calculate the HD function for the stochastic background with a power law spectrum  $\parallel$ . Thus, we will calculate the Hellings-Downs function via numerical simulations, while the induced signal power, i.e.  $C(\theta = 0)$ , is calculated analytically to guide the physical intuition.

For a stochastic GW background, these metric perturbations are a superposition of monochromatic GWs with random phase and amplitude, and can be written as

$$h_{ij}(t, r^i) = \sum_P \int_{-\infty}^{\infty} df_g \int d\Omega h^P(f_g, \hat{\mathbf{e}}_z) \epsilon_{ij}^P(\hat{\mathbf{e}}_z) e^{i[\omega_g t - \mathbf{k}_g(\omega_g) \cdot \mathbf{r}]}, \quad (7)$$

$\parallel$  One can analytically calculate the HD function for the monochromatic component of the stochastic background. However the results are too lengthy to be really practically useful.

where  $f_g = \omega_g/2\pi$  is the GW frequency,  $\Omega$  is solid angle, spatial indices  $i, j$  run from 1 to 3, and  $h^P$  is the amplitude of the GW propagating in the direction of  $\hat{\mathbf{e}}_z$  per unit solid angle, per unit frequency interval, in polarization state  $P$ , i.e. the six states  $+, \times, b, l, sn, se$  defined in Lee et al. (2008). The basis tensors for these polarization are  $\epsilon_{ij}^P$  are

$$\begin{aligned}\epsilon_{ab}^+ &= \hat{\mathbf{e}}_{xa}\hat{\mathbf{e}}_{xb} - \hat{\mathbf{e}}_{ya}\hat{\mathbf{e}}_{yb}, \\ \epsilon_{ab}^\times &= \hat{\mathbf{e}}_{xa}\hat{\mathbf{e}}_{yb} + \hat{\mathbf{e}}_{ya}\hat{\mathbf{e}}_{xb}, \\ \epsilon_{ab}^b &= \hat{\mathbf{e}}_{xa}\hat{\mathbf{e}}_{xb} + \hat{\mathbf{e}}_{ya}\hat{\mathbf{e}}_{yb}, \\ \epsilon_{ab}^{sn} &= \hat{\mathbf{e}}_{xa}\hat{\mathbf{e}}_{zb} + \hat{\mathbf{e}}_{za}\hat{\mathbf{e}}_{xb}, \\ \epsilon_{ab}^{se} &= \hat{\mathbf{e}}_{ya}\hat{\mathbf{e}}_{zb} + \hat{\mathbf{e}}_{za}\hat{\mathbf{e}}_{yb}, \\ \epsilon_{ab}^l &= \hat{\mathbf{e}}_{za}\hat{\mathbf{e}}_{zb}.\end{aligned}\tag{8}$$

If the GW background is isotropic, stationary and independently polarized, we can define the characteristic strain  $h_c^P$  according to

$$\langle h^P(f, \hat{\mathbf{e}}_z) h^{P'\star}(f', \hat{\mathbf{e}}_z') \rangle = \frac{1}{4\pi} \delta(f - f') \delta(\hat{\mathbf{e}}_z - \hat{\mathbf{e}}_z') \delta_{PP'} \frac{|h_c^P|^2}{\eta(P)f}.\tag{9}$$

where  $\star$  stands for the complex conjugate and  $\langle \rangle$  is the statistical ensemble average. The symbol  $\delta_{PP'}$  is the Kronecker delta for polarization states;  $\delta_{PP'} = 0$  when  $P$  and  $P'$  are different, and  $\delta_{PP'} = 1$ , when  $P$  and  $P'$  are the same. If we define  $\eta(P) \equiv 4$ , for  $P = +, \times, b, sn, se$ , and  $\eta(P) \equiv 2$ , for  $P = l$ , one can show that

$$\langle h_{ab}(t) h_{ab}(t) \rangle = \sum_{P=+, \times} \int_0^\infty \frac{|h_c^P|^2}{f_g} df_g.\tag{10}$$

We use Monte-Carlo simulations to determine the shape of the HD function for GW backgrounds with a power-law spectra. In the simulations for  $C(\theta)$ , we randomly choose pulsars from an isotropic distribution over sky positions. We then hold constant these pulsar positions and calculate the angular separation  $\theta$  between every pair of pulsars. Next, to simulate the power-law GW background, we generate  $10^4$  monochromatic waves, choosing random phase, and choosing the amplitude according to the power-law such that the characteristic strain  $h_c = A_c(f/f)^\alpha$ , where we take  $\alpha = 2/3$  for practical purposes (Phinney, 2001). The timing residuals are calculated using equation (2). Then, the cross power,  $C(\theta)$ , between pulsar pairs is calculated. We repeat such processes and average over the angular dependent cross-power  $C$  until its change is less than 0.1%. From cross power  $C(\theta)$ , we calculate the Hellings-Downs curve according to  $H(\theta) = C(\theta)/C(0)$ , where  $C(0)$  is just the power of the GW induced signal of single pulsar. The Hellings-Downs curves for all six polarization with different graviton masses are plotted in Figure 1.

We now analytically calculate the power spectrum of pulsar timing residuals induced by the stochastic GW background. One can show that power spectrum of the induced pulsar timing residuals is

$$S_R(f_g) = \int d\Omega \frac{|h_c^P|^2}{16\pi f_g} \left[ \frac{\epsilon_{ij}^P A^{ij}}{\omega_g + c\mathbf{k}_g \cdot \hat{\mathbf{n}}} \right]^2 \left[ 1 - \cos \left( \frac{D}{c} (\omega_g + c\mathbf{k}_g \cdot \hat{\mathbf{n}}) \right) \right].\tag{11}$$

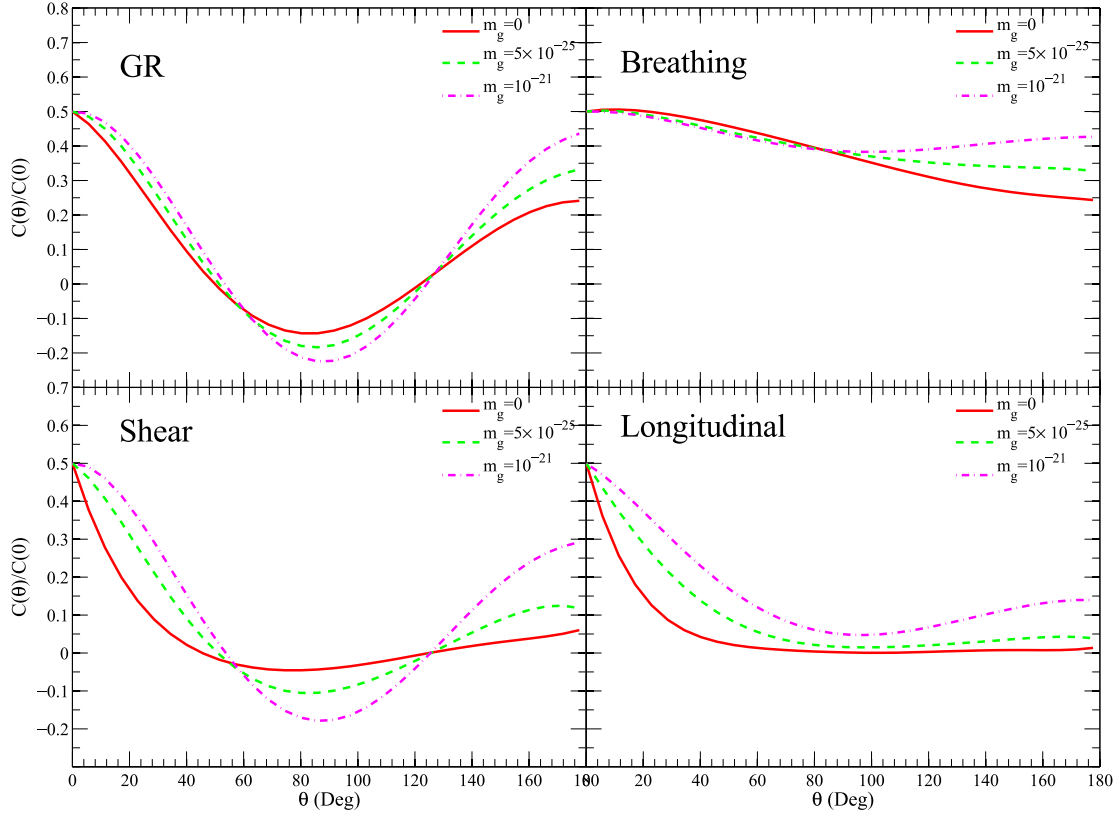


**Figure 1.** The HD correlation functions of all six polarization modes. The solid, dashed, and dot-dashed curves are for graviton mass of 0,  $5 \times 10^{-25}$ , and  $10^{-22}$  eV respectively. In the calculation, we assume that the total observing length is 10 years, while the cadence is two weeks. The distance of the pulsars are all assumed to be 1 kpc. One can clearly see the graviton mass dependence of the HD function of each polarization modes.

After integrating out the solid angle  $d\Omega$  in equation (11), one can show that ¶

$$S_R(f) = \sum_P \frac{|h_c^P|^2}{24\pi^2 f^3} F^P. \quad (12)$$

Here the  $F^P$  is the amplifying factor of the pulsar timing response to the polarization mode  $P$  normalized to the massless GR case. The amplifying factors depend on the

¶ These results are partly due to the independent polarization assumption, which assumes no correlation between the polarizations via  $\delta_{PP'}$ , as in equation (9). However only an extra term involving the longitudinal and breathing modes, the  $\langle h^b h^l \rangle$ , will appear, if we further allow for the cross-correlation of the modes, i.e. the ‘circular’ polarization. Interestingly, the correlation function and power of such term are identical to that of shear modes.



mass of graviton and the pulsar distances as

$$F^{+, \times} = \int_{-1}^1 \frac{3(1-\mu^2)^2 \sin^2 \left[ \frac{1}{2}(\zeta\mu\Phi + \Phi) \right]}{4(\zeta\mu + 1)^2} d\mu, \quad (13)$$

$$F^b = 2F^{+, \times}, \quad (14)$$

$$F^{sn, se} = \int_{-1}^1 \frac{3\mu^2(1-\mu^2) \sin^2 \left[ \frac{1}{2}(\zeta\mu\Phi + \Phi) \right]}{(\zeta\mu + 1)^2} d\mu, \quad (15)$$

$$F^l = \int_{-1}^1 \frac{3\mu^4 \sin^2 \left[ \frac{1}{2}(\zeta\mu\Phi + \Phi) \right]}{(\zeta\mu + 1)^2} d\mu, \quad (16)$$

where  $\zeta \equiv \sqrt{1 - (\omega_{\text{cut}}/\omega_g)^2}$ , and  $\Phi = D\omega_g/c$  is the pulsar distance in unit of GW wave length<sup>+</sup>. Although the amplifying factor can be integrated analytically (given in the Appendix A), the exact form is complex and awkward to use. Here we check the behavior of  $F^P$  in two limiting case  $\zeta = 0$  and  $\zeta = 1$ . The Cases  $\zeta = 1$  corresponds to the massless graviton, while  $\zeta = 0$  is the situation where the GW wave vector vanishes, i.e. the corresponding graviton momentum is zero. One can show that

$$F^{+, \times} = \begin{cases} 1 + \mathcal{O}\left(\frac{1}{\Phi^2}\right) & \text{when } \zeta = 1 + \mathcal{O}\left(\frac{1}{\Phi^2}\right), \\ \frac{2}{5}(1 - \cos \Phi), & \text{when } \zeta = 0, \end{cases} \quad (17)$$

$$F^b = 2F^{+, \times}, \quad (18)$$

$$F^{sn/se} = \begin{cases} 3 \log \Phi + 3\gamma - 7 + \log 8 + \mathcal{O}\left(\frac{1}{\Phi}\right) & \text{when } \zeta = 1, \\ \frac{2}{5}(1 - \cos(\Phi)), & \text{when } \zeta = 0, \end{cases} \quad (19)$$

$$F^l = \begin{cases} \frac{3\pi\Phi}{4} - 6 \log \Phi - 6\gamma + \frac{37}{4} - 3 \log 4 + \mathcal{O}\left(\frac{1}{\Phi}\right), & \text{when } \zeta = 1, \\ \frac{3}{5}(1 - \cos \Phi), & \text{when } \zeta = 0, \end{cases} \quad (20)$$

where the symbol  $\mathcal{O}$  means “the order of”. Here we assumes the short-wave approximation that  $\Phi \gg 1$ , i.e. the pulsar distance is much larger than the zero mass wavelength of GW. Such an assumption is valid for most PTA applications, where  $\Phi \simeq 10^3$ .

One interesting effect is that the cross power of pulsar pairs separated by  $180^\circ$ , the  $C(180^\circ)$ , also gain an extra distance dependent amplification for the longitudinal mode. One can show that

$$C^l(180^\circ) = \frac{|h_c^P|^2}{192\pi^2 f^3} [3 \log \Phi + 3\gamma - 8 + \log 8]. \quad (21)$$

However, due to the logarithmic dependence on  $\Phi$ , the effect of boosting the PTA sensitivity is rather limit compared to the case of  $\theta \simeq 0$ .

Another thing worth mentioning is that the Hellings and Downs curves have very similar shape at the cut-off frequency limit, i.e.  $\zeta = 0$ . In this case, the integrations in equation (13)–equation (16) are very simple, and we can derive the analytic form that

$$C^{+, \times}(\theta)/C^{+, \times}(0) = \frac{1}{4}(1 + 3 \cos 2\theta), \quad (22)$$

<sup>+</sup>  $\Phi$  is just the pulsar distance. It is not the phase difference between the pulsar and earth term, which is  $\Delta\Phi = D/c(\omega_g + \mathbf{c}\mathbf{k}_g \cdot \hat{\mathbf{n}})$ .

$$C^b(\theta)/C^b(0) = \frac{1}{8} (7 + \cos 2\theta), \quad (23)$$

$$C^{sn,se}(\theta)/C^{sn,se}(0) = C^{+,\times}(\theta)/C^{+,\times}(0), \quad (24)$$

$$C^{+,\times}(\theta)/C^{+,\times}(0) = \frac{1}{3} (2 + \cos 2\theta). \quad (25)$$

All the HD function are practically identical to each other, since they only differ by constant offsets, to which PTAs are not sensitive, because of the clock noise. Thus, discrimination between the polarization modes could be difficult, if the graviton mass is not negligibly small.

## 5. Discussion and Conclusion

In this paper, we reviewed the current efforts to test alternative gravity theories by measuring the mass of the graviton and detecting alternative polarization modes of GWs, in the context of PTA experiments. We explained the method to measure the graviton mass or detect alternative GW polarization by measuring the cross-correlation function of pulsar timing residuals, i.e. HD functions. This method is different from the techniques for single GW sources, where one can model the waveform and compare it to the observations. We do not need to model the waveform for these PTA experiments. Thus the gravity test will be independent of the models of GW sources or generation mechanisms.

We have also extended previous calculations for the Hellings-Downs function to the most general case, where one allows for the alternative polarization modes as well as dispersion due to a massive graviton. Such the extension is driven by the consideration that alternative polarization modes usually originate from gauge symmetry breaking, which could be induced by a graviton mass. Because of such connections between the massive graviton and polarization modes, it is necessary to consider both effects at the same time, when trying to test gravity theories using PTA data.

One particular interesting case is the longitudinal modes. It is known that an large amplifying factor, e.g. the  $3\pi\Phi/4$  in equation (20). Most of the pulsars in PTA has distance of a few thousand light years. This makes the amplifying factors be about  $10^4$ . Several authors (Lee et al., 2008; Alves and Tinto, 2011; Chamberlin and Siemens, 2012) have realized this could be a very good opportunity to put tight bounds on the amplitude of longitudinal modes. However, these modes are likely to be a massive modes and, according to equation (20), the amplifying factor drops to order of unity, when approaching the cut-off frequency. Thus, a null detection of longitudinal modes should not be just interpreted as the upper bounds for the GW amplitude. The null detection can be also be explained by a small graviton mass. A similar effect is seen for the shear modes. However the effect is not that dramatic, because the amplifying factor is proportional to the logarithmic of the pulsar distance, which only increases the pulsar timing response by a order of magnitude. The drop-off of the amplifying factor by the graviton mass is natural. When the GW frequency approaches the cut-off frequency, the wave vector vanishes and the wavelength becomes arbitrarily large. This effectively

stops the spatial oscillation of the GW, reduces the difference between pulsar and Earth term, and brings down the amplifying factors.

We have shown that the Hellings-Downs function is not a single function. They are, in fact, six sets of functions depending on the polarization and graviton mass. In this paper, we did not go into the details of the related signal detection and discrimination problems, as they beyond the scope of this paper. On the other hand, from simulations, forty to a few hundred pulsars are required to differentiate the difference in Hellings-Downs functions via a correlation analysis (Lee et al., 2008, 2010). In this way, testing gravity theories using PTAs would be, unfortunately, beyond current ability of PTAs. However, the number of pulsars ( $N$ ) one can time to a given accuracy is proportional to the fourth power of the telescope effective diameter according to the radiometer equation. In this way, we would expect that future telescopes with larger effective diameters, such as the Large European Array for Pulsars (Stappers et al. 2009, Kramer & Champion, 2013, in this volume), the Five-hundred-meter Aperture Spherical Radio Telescope (Nan et al., 2006; Smits et al., 2009) and the Square Kilometer Array (SKA, Lazio, 2013, in this volume) will offer unique opportunities to find and time these pulsars; and to detect the GW background and test gravity theories in the radiative regime.

## **Acknowledgments**

KJL gratefully acknowledges support from the ERC Advanced Grant ‘LEAP’, Grant Agreement Number 227947 (PI Michael Kramer). The author thank Lijing Shao, C. M. F. Mingaralli, and members in the EPTA data analysis group for useful discussions. The author also thank D. Champion, M. Kramer for reading the manuscript and for their valuable comments.

## Appendix A. The full form of amplifying factors

Integration of equation (13)–(16) can be performed analytically using the Sine-Cosine integrals, where one has

$$\begin{aligned}
 F^{+, \times} &= \frac{W}{4\zeta^5} + \frac{3 \cos \Phi \sin(\zeta \Phi)}{2\zeta^5 \Phi^3} - \frac{3(\sin \Phi \sin(\zeta \Phi) + \zeta \cos \Phi \cos(\zeta \Phi))}{2\zeta^5 \Phi^2} \\
 &+ \frac{3(\zeta^2 - 3) \cos \Phi \sin(\zeta \Phi) + 6\zeta \sin \Phi \cos(\zeta \Phi)}{4\zeta^5 \Phi} \\
 &+ \frac{3(\zeta^2 - 1)^2 \Phi [\text{Si}(\zeta \Phi + \Phi) - \text{Si}(\Phi - \zeta \Phi)]}{8\zeta^5}, \tag{A.1}
 \end{aligned}$$

$$F^b = 2F^{+, \times}, \tag{A.2}$$

$$\begin{aligned}
 F^{sn, se} &= \frac{V}{\zeta^5} - \frac{6 \cos \Phi \sin(\zeta \Phi)}{\zeta^5 \Phi^3} + \frac{6(\sin \Phi \sin(\zeta \Phi) + \zeta \cos \Phi \cos(\zeta \Phi))}{\zeta^5 \Phi^2} \\
 &+ \frac{9 \cos \Phi \sin(\zeta \Phi) - 6\zeta \sin \Phi \cos(\zeta \Phi)}{\zeta^5 \Phi} \\
 &+ \frac{3(\zeta^2 - 1) \Phi [\text{Si}(\zeta \Phi + \Phi) - \text{Si}(\Phi - \zeta \Phi)]}{2\zeta^5}, \tag{A.3}
 \end{aligned}$$

$$\begin{aligned}
 F^l &= \frac{U}{2\zeta^5 (\zeta^2 - 1)} + \frac{3 \cos \Phi \sin(\zeta \Phi)}{\zeta^5 \Phi^3} - \frac{3(\sin \Phi \sin(\zeta \Phi) + \zeta \cos \Phi \cos(\zeta \Phi))}{\zeta^5 \Phi^2} \\
 &+ \frac{6\zeta \sin \Phi \cos(\zeta \Phi) - 3(\zeta^2 + 3) \cos \Phi \sin(\zeta \Phi)}{2\zeta^5 \Phi} \\
 &+ \frac{3\Phi [\text{Si}(\zeta \Phi + \Phi) - \text{Si}(\Phi - \zeta \Phi)]}{4\zeta^5}, \tag{A.4}
 \end{aligned}$$

Here the  $U, V$ , and  $W$  are defined as

$$\begin{aligned}
 U &= 6(\zeta^2 - 1) [\text{Ci}(\zeta \Phi + \Phi) - \text{Ci}(\Phi - \zeta \Phi)] \\
 &+ \zeta^5 + 8\zeta^3 - 12(\zeta^2 - 1) \tanh^{-1} \zeta + 3 \sin \Phi \sin(\zeta \Phi) \\
 &+ 3\zeta \cos \Phi \cos(\zeta \Phi) - 12\zeta, \tag{A.5}
 \end{aligned}$$

$$\begin{aligned}
 V &= 3(\zeta^2 - 2) [\text{Ci}(\zeta \Phi + \Phi) - \text{Ci}(\Phi - \zeta \Phi)] + 2\zeta(\zeta^2 - 6) \\
 &- 6(\zeta^2 - 2) \tanh^{-1} \zeta + 3 \sin(\Phi) \sin(\zeta \Phi) + 3\zeta \cos(\Phi) \cos(\zeta \Phi), \tag{A.6}
 \end{aligned}$$

$$\begin{aligned}
 W &= 6(\zeta^2 - 1) [\text{Ci}(\Phi - \zeta \Phi) - \text{Ci}(\zeta \Phi + \Phi)] + 3(\zeta^2 - 1) \sin \Phi \sin(\zeta \Phi) \\
 &+ 4(-2\zeta^3 + 3(\zeta^2 - 1) \tanh^{-1} \zeta + 3\zeta) \\
 &+ 3\zeta(\zeta^2 - 1) \cos \Phi \cos(\zeta \Phi). \tag{A.7}
 \end{aligned}$$

These equations are the exact calculation for the amplification factors, i.e. no assumption such as  $\Phi \gg 1$  are made. In this way, these equation also valid to calculate the timing residual with the much lower frequencies compared to the case of equation (17)–(20).

## References

- Alves M E D S and Tinto M 2011 *Phys. Rev. D* **83**(12), 123529.
- Anholm M, Ballmer S, Creighton J D E, Price L R and Siemens X 2009 *Phys. Rev. D* **79**(8), 084030.
- Arun K G and Will C M 2009 *Classical and Quantum Gravity* **26**(15), 155002.
- Babak S and Sesana A 2012 *Phys. Rev. D* **85**(4), 044034.
- Boyle L and Pen U L 2012 *Phys. Rev. D* **86**(12), 124028.
- Burt B J, Lommen A N and Finn L S 2011 *ApJ* **730**, 17.
- Chamberlin S J and Siemens X 2012 *Phys. Rev. D* **85**(8), 082001.
- Cordes J M and Jenet F A 2012 *ApJ* **752**, 54.
- Cordes J M and Shannon R M 2012 *ApJ* **750**, 89.
- Damour T, Kogan I I and Papazoglou A 2003 *Phys. Rev. D* **67**(6), 064009–+.
- Deffayet C, Dvali G, Gabadadze G and Vainshtein A 2002 *Phys. Rev. D* **65**(4), 044026–+.
- Deng X and Finn L S 2011 *MNRAS* **414**, 50–58.
- Detweiler S 1979 *ApJ* **234**, 1100–1104.
- Dirac P A M 1984 *International Journal of Theoretical Physics* **23**, 677–681.
- Eardley D M, Lee D L and Lightman A P 1973 *Phys. Rev. D* **8**(10), 3308–3321.
- Ellis J A, Jenet F A and McLaughlin M A 2012 *ApJ* **753**, 96.
- Ellis J A, Siemens X and Creighton J D E 2012 *ApJ* **756**, 175.
- Enoki M, Inoue K T, Nagashima M and Sugiyama N 2004 *ApJ* **615**, 19–28.
- Estabrook F B and Wahlquist H D 1975 *General Relativity and Gravitation* **6**, 439–447.
- Finn L S and Lommen A N 2010 *ApJ* **718**, 1400–1415.
- Finn L S and Sutton P J 2002 *Phys. Rev. D* **65**(4), 044022–+.
- Fomalont E, Kopeikin S, Lanyi G and Benson J 2009 *ApJ* **699**, 1395–1402.
- Goldhaber A S and Nieto M M 2010 *Reviews of Modern Physics* **82**, 939–979.
- Hellings R W and Downs G S 1983 *ApJ* **265**, L39–L42.
- Iwasaki Y 1970 *Phys. Rev. D* **2**, 2255–2256.
- Jaffe A H and Backer D C 2003 *ApJ* **583**, 616–631.
- Jenet F A, Hobbs G B, Lee K J and Manchester R N 2005 *ApJL* **625**, L123–L126.
- Jenet F A, Lommen A, Larson S L and Wen L 2004 *ApJ* **606**, 799–803.
- Kashiyama K and Seto N 2012 *MNRAS* **426**, 1369–1373.
- Lee K J, Bassa C G, Janssen G H, Karuppusamy R, Kramer M, Smits R and Stappers B W 2012 *Mnras* **423**, 2642–2655.
- Lee K J, Jenet F A and Price R H 2008 *ApJL* **685**, 1304–1319.

- Lee K J, Wex N, Kramer M, Stappers B W, Bassa C G, Janssen G H, Karuppusamy R and Smits R 2011 *MNRAS* **414**, 3251–3264.
- Lee K, Jenet F A, Price R H, Wex N and Kramer M 2010 *ApJ* **722**, 1589–1597.
- Lommen A N 2012 in ‘American Astronomical Society Meeting Abstracts #219’ Vol. 219 of *American Astronomical Society Meeting Abstracts* p. 108.03.
- Mingarelli C M F, Grover K, Sidery T, Smith R J E and Vecchio A 2012 *Physical Review Letters* **109**(8), 081104.
- Mirshekari S, Yunes N and Will C M 2012 *Phys. Rev. D* **85**(2), 024041.
- Nan R, Wang Q, Zhu L, Zhu W, Jin C and Gan H 2006 *Chinese Journal of Astronomy and Astrophysics Supplement* **6**(2), 020000–310.
- Phinney E S 2001 *preprint*, *arxiv: 0108028* .
- Ravi V, Wyithe J S B, Hobbs G, Shannon R M, Manchester R N, Yardley D R B and Keith M J 2012 *ApJ* **761**, 84.
- Sanidas S A, Battye R A and Stappers B W 2012 *Phys. Rev. D* **85**(12), 122003.
- Sazhin M V 1978 *Soviet Astronomy* **22**, 36–38.
- Sesana A, Haardt F, Madau P and Volonteri M 2004 *ApJ* **611**, 623–632.
- Sesana A and Vecchio A 2010 *Phys. Rev. D* **81**(10), 104008.
- Sesana A, Vecchio A and Colacino C N 2008 *MNRAS* **390**, 192–209.
- Sesana A, Vecchio A and Volonteri M 2009 *MNRAS* **394**, 2255–2265.
- Seto N 2009 *MNRAS* **400**, L38–L42.
- Smits R, Lorimer D R, Kramer M, Manchester R, Stappers B, Jin C J, Nan R D and Li D 2009 *A&A* **505**, 919–926.
- Stappers B, Vlemmings W and Kramer M 2009 in ‘Proceedings of the 8th International e-VLBI Workshop. 22-26 June 2009. Madrid, Spain’ p. 20.
- Stavridis A and Will C M 2009 *Phys. Rev. D* **80**(4), 044002–+.
- Vainshtein A I 1972 *Physics Letters B* **39**, 393–394.
- van Dam H and Veltman M 1970 *Nuclear Physics B* **22**, 397–411.
- van Haasteren R and Levin Y 2010 *MNRAS* **401**, 2372–2378.
- van Haasteren R, Levin Y, McDonald P and Lu T 2009 *MNRAS* **395**, 1005–1014.
- Verbiest J P W, Bailes M, Coles W A, Hobbs G B, van Straten W, Champion D J, Jenet F A, Manchester R N, Bhat N D R, Sarkissian J M, Yardley D, Burke-Spolaor S, Hotan A W and You X P 2009 *MNRAS* **400**, 951–968.
- Visser M 1998 *General Relativity and Gravitation* **30**, 1717–1728.
- Wen Z L, Liu F S and Han J L 2009 *ApJ* **692**, 511–521.
- Will C 2006 *Living Reviews in Relativity* **9**, 3.
- Will C M 1998 *Phys. Rev. D* **57**, 2061–2068.
- Wyithe J S B and Loeb A 2003 *ApJ* **590**, 691–706.

- Yardley D R B, Coles W A, Hobbs G B, Verbiest J P W, Manchester R N, van Straten W, Jenet F A, Bailes M, Bhat N D R, Burke-Spolaor S, Champion D J, Hotan A W, Osłowski S, Reynolds J E and Sarkissian J M 2011 *MNRAS* **414**, 1777–1787.
- Zakharov V I 1970 *ZhETF Pis ma Redaktsiiu* **12**, 447–+.